Research Square

Preprints are preliminary reports that have not undergone peer review.
They should not be considered conclusive, used to inform clinical practice,
or referenced by the media as validated information.

Evaluation of the Metal Artifact Caused by Two Different Amalgams in Cone Beam Computed Tomography Images

Atena Jamali
Student Research Committee, Babol University of Medical Sciences
Ehsan Moudi
mubabol2000@gmail.com
Oral Health Research Center, Health Research Institute, Babol University of Medical Sciences
Sina Haghanifar
Oral Health Research Center, Health Research Institute, Babol University of Medical Sciences
Maryam Johari
Oral Health Research Center, Health Research Institute, Babol University of Medical Sciences
Homayoon Alaghehmand
Dental Materials Research Center, Health Research Institute, Babol University of Medical Sciences
Ali Bijani
Social Determinants of Health Research Center, Health Research Institute, Babol University of Medical Sciences
Ariana Rezaei Majd
Dental Materials Research Center, Health Research Institute, Babol University of Medical Sciences

Research Article

Keywords: Artifact, Cone-Beam Computed Tomography, Dental Amalgam

Posted Date: November 18th, 2026

DOI: https://doi.org/10.21203/rs.3.rs-11254634/v1

License: This work is licensed under a Creative Commons Attribution 4.0 International License.
Read Full License

Additional Declarations: No competing interests reported.

Evaluation of the Metal Artifact Caused by Two Different Amalgams in Cone Beam Computed Tomography Images

Atena Jamali[1], Ehsan Moudi [2*], Sina Haghanifar[2], Maryam Johari[3], Homayoon Alaghehmand[4], Ali Bijani[5,] Ariana Rezaei Majd[6]

1: Postgraduate Student of Oral and Maxillofacial Radiology, Student Research Committee, Babol University of Medical Sciences, Babol, Iran.
2: Professor of Oral and Maxillofacial Radiology, Department of Oral and Maxillofacial Radiology, School of Dentistry, Oral Health Research Center, Health Research Institute, Babol University of Medical Sciences, Babol, Iran.
3: Assistant Professor of Oral and Maxillofacial Radiology, Department of Oral and Maxillofacial Radiology, School of Dentistry, Oral Health Research Center, Health Research Institute, Babol University of Medical Sciences, Babol, Iran.
4: Professor of Restorative Dentistry, Department of Restorative Dentistry, School of Dentistry, Dental Materials Research Center, Health Research Institute, Babol University of Medical Sciences, Babol, Iran.
5: Associate Professor, Social Determinants of Health Research Center, Health Research Institute, Babol University of Medical Sciences, Babol, Iran.
6: Doctor of Dental Surgery, Dental Materials Research Center, Health Research Institute, Babol University of Medical Sciences, Babol, Iran.
[*]**Corresponding Author:** Ehsan Moudi, School of Dentistry, Babol University of Medical Sciences, GanjAfrooz Ave, Babol, Iran. Tel & Fax: +98-11-322-91408 Email: mubabol2000@gmail.com ORCID ID: 0009-0003-4042-0827

Abstract

Background: The aim of this study was to evaluate and compare the intensity of the artifacts produced by two different types of dental amalgam restorations using two cone-beam computed tomography (CBCT) unite.

Methods: For this experimental study, three dry human mandibles were selected. Two different types of amalgam (A: high-silver B: low-silver) were prepared in

standardized dimensions of 8*8*8 mm and placed in the empty sockets of lateral incisor and first molar teeth were stabilized using dental wax. Each mandible was placed in the phantom simulating soft tissue and occlusal plane was adjusted parallel to the horizontal plane. The CBCT images were taken with two different CBCT devices and two different resolutions. Gray values and the contrast noise ratio (CNR) was calculated. The CNR values of images were analyzed based on the amalgam type, image resolution, jaw region (anterior vs posterior), units parameters, and the results were statistically analyzed using the paired t-test.

Results: Depending on the CBCT device, the CNR values for A and B amalgams are completely different. The CNR values of both amalgam types were significantly higher under high resolution settings compared to standard resolution. However, no significant difference in CNR values were observed between the anterior and posterior regions of the mandible.

Conclusions: The extent of metal artifacts in CBCT images is significantly influenced by the type of amalgam, scanning parameters, and image resolution. Higher resolution led to an increase in CNR (p-value = 0.000). However, the location of the amalgam (anterior or posterior regions of the mandible) had no significant effect on the artifact level. These findings can contribute to improving CBCT image quality in the presence of metallic restorations.

Keywords: Artifact, Cone-Beam Computed Tomography, Dental Amalgam.

Introduction

Cone Beam Computed Tomography (CBCT) has become an invaluable tool in dental imaging, offering high-resolution, three-dimensional representations of the oral cavity, particularly in endodontics, implantology, and maxillofacial diagnosis, due to its high-resolution 3D imaging and relatively low radiation dose compared to conventional CT scans(1, 2). Despite its numerous advantages, artifacts decrease the quality of CBCT images. These artifacts often originate from high-density dental materials, such as amalgam restorations, crowns, orthodontic appliances ,and root fillings can severely compromise diagnostic accuracy by distorting adjacent structures and masking pathological findings(3).Metal artifacts are primarily caused by the high atomic number and density of metallic objects, which lead to complex physical interactions with X-ray beams, such as beam hardening, scatter, and photon starvation(4, 5). Beam hardening is more noticeable on CBCT images due to the heterochromatic nature and lower kVp energy of CBCT X-ray beams compared with medical CT(6).Beam hardening occurs when lower-energy photons are absorbed more readily than higher-energy ones as the X-ray beam traverses through dense metal, resulting in two distinct artifact manifestations: streaking (dark bands) and cupping artifacts (distortion of the metal structure) (7). Many variables are involved with the incidence of artifacts, such as exposure conditions, pixel size, and field of view (FOV)(8, 9). There are some studies

investigation the use of artifact reduction algorithm (10, 11). Although these algorithms can partially reduce the incidence of artifacts, the details around the metal-tissue interface, as the main region of interest (ROI), may still remain unobservable to the clinicians (12). Therefore, the effects of factors capable of reducing metal-related artifacts in CBCT imaging should be assessed. The aim of this study is to assess and compare the metal artifacts produced by two different types of amalgam restorations in CBCT images, with the goal of enhancing artifact management strategies in clinical practice.

Materials and Methods

In this study used three intact dry human mandibles with empty sockets at lateral incisor and first molar sites, obtained from the Anatomy Department of Babol University of Medical Sciences which are used for scientific research and no patient have been involved in this study. Ethical approval for the study was obtained from the Clinical Research Ethics Committee of the Faculty of Dentistry at Babol University of Medical Sciences (IR.MUBABOL.HRI.REC.1403.125).

Two different types of encapsulated dental amalgam, with varying silver content, were used in this study:

1. Sepehr Amalgam (Sepehr Dental Co., Tehran, Iran): composed of 45% silver, 30% tin, and 25% copper, with lathe-cut particle type; mixing time :7- 30 seconds at 4000 rpm.

2. Solaloy Amalgam (Solaloy, London, England): composed of 68.4% silver, 26.3% tin, and 4.7% copper, also with lathe-cut particles; mixing time: 7-15 seconds at 4200 rpm. An amalgamator device (YG200, RIXI, Guangdong, China) was used for mixing the amalgam capsules.

To standardize the amalgam boxes, a mold with dimensions of 8 × 8 × 8 mm was fabricated. The mixed amalgam was packed into the mold to form uniform cubic shapes simulating amalgam boxes. For placement, dental wax was first inserted into the empty sockets, and then the preformed amalgam boxes were positioned and fixed on top of the wax. Each amalgam box was carefully centered within the socket such that the distance between the box and both the buccal and lingual plates was equal.CBCT images were acquired using two CBCT units X MIND (ACTEON, Olgiate olona, Italy) and 5G (Newtom, Verrona, Italy) at two different resolutions (high and standard) in the presence and absence of fixtures (as the case and control groups, respectively). The X MIND scan parameters were set as follows: 90 kVp, current of 8 mA, FOV of 11×8 cm and pixel size of 150 μ at standard resolution and 100 μ at high resolution. The 5G scan parameters were set as follows: 110 kVp, current of 10 mA, FOV of 12×8 cm and the pixel size of 150 μ at standard resolution and 75 μ at high resolution. In order to best simulate alveolar soft tissue during exposure,the mandibles placed inside a water-filled plastic box to cover the area of interest(6)(Figure1).The XMIND images were

analyzed with OnDemand 3D Dental, and 5G images were analyzed with NNT software.

First, the mandibles with empty sockets in the lateral and first molar regions were placed inside the plastic phantom filled with water. Then, CBCT images were taken at standard and high resolution, using XMIND and 5G units (control group). Next, the Sepehr amalgam cubes (8 × 8 × 8 mm) were placed in the lateral and first molar sockets, fixed by wax and scanned using both devices and both resolution settings. The same procedures were conducted with the Solaloy amalgam cubes (8 × 8 × 8 mm). In total, 36 CBCT scans were acquired (24 scans in the case group and 12 scans in the control group). To standardize ROI positions and include the artifact areas, the following method was used: In the axial view of each section, a line was drawn from the center of the amalgam box along the longitudinal axis of the alveolar ridge ;then, a perpendicular line was drawn from this axis.Additionally a semicircle(1.5 cm in diameter) was drawn from the center of the amalgam box, resulting in a square (25×25 pixels), as ROI, at the intersection of semicircle and line(Figure 2)(13). The gray values in these areas were calculated and placed in following formula to obtain the CNR values (14).

$$CNR = \frac{|\text{Mean}_{\text{Amalgam}} - \text{Mean}_{\text{Control}}|}{\sqrt{SD^2_{\text{Amalgam}} + SD^2_{\text{Control}}}}$$

*CNR = Contrast to Noise Ratio



FIGURE1: Soft tissue simulation with water.

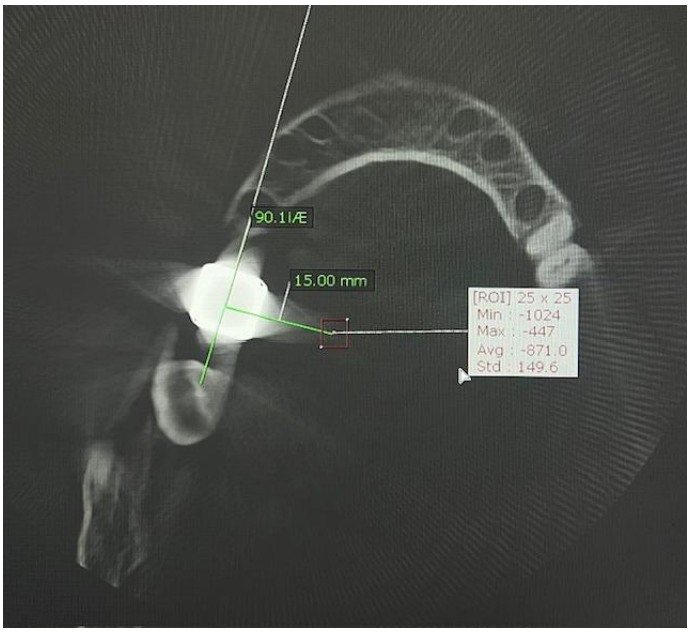


FIGURE2: CNR Calculation Method in Mandibulary posterior region of Solaloy.

The mean, standard deviation, and standard error of CNR values of CBCT images were calculated and reported based on type of amalgam (Sepehr-Sollaloy), anterior-posterior mandibular region and resolution(high-standard), size (anterior-posterior).

The statistical comparison of CNR values by dual-mode variables (amalgam type, posterior or anterior mandibular region, resolution) was done using the paired t-test.

Results

In contrast to XMIND, the mean CNR values of Sepehr amalgam in 5G were higher than Solaloy (Table1-figure3).

However, there was not any significant difference between anterior and posterior regions of mandible for Solaloy and Sepehr amalgam in terms of the CNR values(Table1-figure3).

Moreover, significant difference in the CNR values overall,were found between high and standard resolutions (Table2) .

Nevertheless, when comparing CNR values of Solaloy and Sepehr amalgams separately across high and standard resolutions within each device (XMIND and 5G), no statistically significant difference was observed.(Table 3-figure3)

Table 1. Measures of central dispersion of CNR values for Solaloy and Sepehr amalgam by unit, and site of mandible.

		Amalgam	Number	Mean	SD*	P value
UNIT	X MIND	Solaloy	12	2/89	3/73	0/018
		Sepehr	12	2/31	2/59	
	5G	Solaloy	12	2/66	2/68	0/047
		Sepehr	12	3/61	3/94	
Site	Anterior	Solaloy	12	3/69	2/91	0/441
	Posterior		12	1/78	2/87	
	Anterior	Sepehr	12	3/71	2/50	0/425
	Posterior		12	1/79	3/40	

*SD: Standard Deviation

Table 2. Measures of central dispersion of CNR values based on resolution.

Resolution	Number	Mean	SD	P value
high	24	3/36	2/65	0/000
standard	24	2/12	3/07	

Table 3. Measures of central dispersion of CNR values for Solaloy and Sepehr amalgam by resolution .

Unit	Amalgam	resolution (voxel size)*	Mean	SD	P value
X MIND	Solaloy	150 100	0/796 1/89	0/22 2/37	0/645
X MIND	Sepehr	150 100	0/658 1/98	1/02 1/86	0/063
5G	Solaloy	100 75	3/72 4/45	3/93 3/07	0/896
5G	Sepehr	100 75	4/197 4/147	4/30 3/146	0/761

*XMIND: high resolution =100 µ, standard resolutin=150µ

5G: high resolution =75 µ, standard resolution =150µ

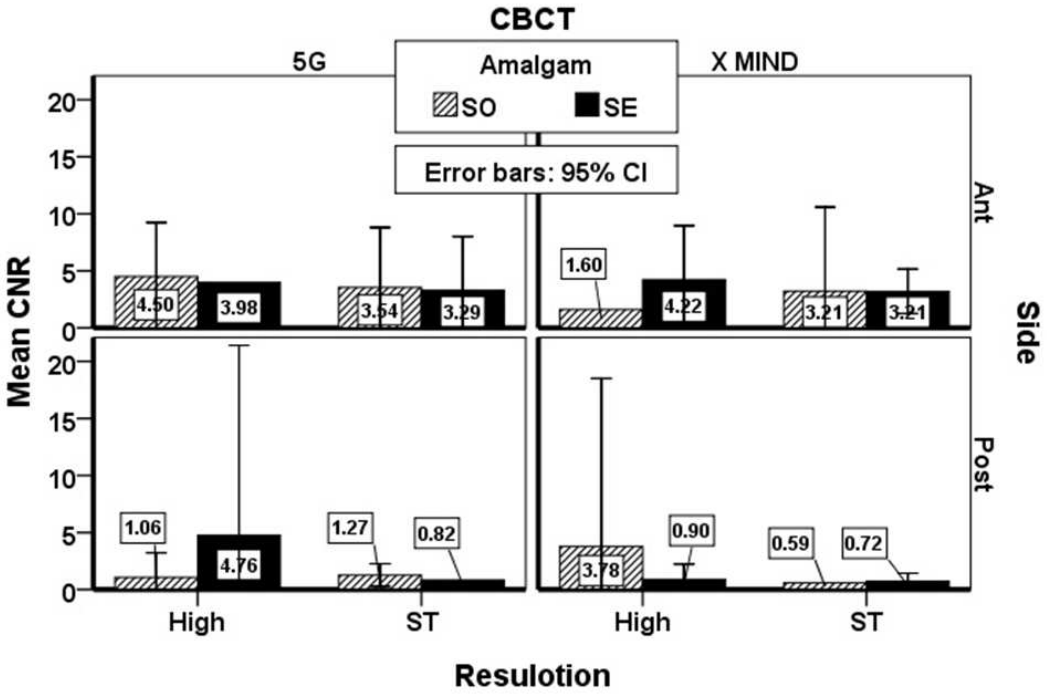


Figure3.Mean CNR Values of CBCT Images by X MIND and 5G, Region of mandible, 2 Resolutions in Solaloy and Sepehr amalgam.

Discussion

Several strategies have been proposed to reduce CBCT artifacts, with varying degrees of success, including the use of a small FOV, antiscatter grids, and voltage adjustment (kVp) and amperage (mA) (2, 15, 16). Applying the MAR algorithm is another proposed strategy for achieving this objective (2). Nevertheless, none of the aforementioned strategies has been able to completely eliminate metal artifacts.

In CBCT, gray values are influenced by several object-related characteristics, particularly its diameter, shape, density, and atomic number (17, 18). Due to the higher density and atomic number compared with soft tissues and bone (19), metals induce beam-hardening artifacts during X-ray imaging (20). To address this issue, this study was among the first to investigate the effects of material composition, exposure parameters, and differences between CBCT units on metal-induced artifacts in CBCT images.

In this study, XMIND and 5G exhibited different CNR values for Sepehr and Solaloy amalgams. In the XMIND, Solaloy amalgam demonstrated a significantly higher CNR than Sepehr amalgam (2.89 vs. 2.31). However, the 5G showed a significantly higher CNR for Sepehr amalgam compared with Solaloy (3.61 vs. 2.66). These variations in artifact severity may be attributed to differences in metal composition, CBCT units, kVp settings, and image-processing software (21). Vahdani et al. investigated CBCT artifacts associated with Roxolid and Zirconia fixtures at different locations and angulations. Their findings indicated that both quality and quantity of artifacts were affected by the implant material and the CBCT unit used, which is partially consistent with the results of our study (13).

CNR values showed no statistically significant differences between the anterior and posterior regions of the mandible, in agreement with the findings reported by Vahdani et al. (39).

In contrast, Alessiana et al. reported greater artifact levels in the mandible than in the maxilla, as well as in the anterior regions compared with the posterior regions. These findings differ from those of the present study and may be explained by variations in bone density and thickness within the mandible (22).

In the current study, CNR values were analyzed across different resolution settings, and the results showed that high-resolution images (with smaller voxel size) had significantly higher CNR compared to standard resolution images (with larger voxel size).

Similarly, Dilek Helvacioglu-Yigit et al. reported comparable findings, indicating that voxel size affects the accuracy of vertical root fracture (VRF) detection in the presence of metal artifacts. Their results demonstrated that images acquired with a 0.25 mm voxel size yielded greater diagnostic accuracy than those obtained with a 0.30 mm voxel size (6). Valizadeh et al. reported that the location of an object within the FOV may influence gray value measurements in tomographic images. Depending on the object's position, the X-ray beam may pass along the longitudinal axis of the maxilla or mandible while simultaneously interacting with adjacent implants, teeth, and surrounding bone, thereby increasing artifact formation.

Another potential explanation for the variation in artifact levels across anatomical regions is the influence of exomass, referring to craniofacial structures located

outside the FOV. In these cases, a substantial volume of patient tissue attenuates the X-ray beam, although its effects are not directly represented in the reconstructed image. Therefore, surrounding anatomical structures, particularly the skull and spine, may affect the calculation of gray values in both the maxilla and mandible (23).

Another potential explanation for the variation in artifact levels across anatomical regions is the influence of exomass, referring to craniofacial structures located outside the FOV. In these cases, a substantial volume of patient tissue attenuates the X-ray beam, although its effects are not directly represented in the reconstructed image. Therefore, surrounding anatomical structures, particularly the skull and spine, may affect the calculation of gray values in both the maxilla and mandible (24).

This study used CNR to assess CBCT image quality (6). Radiographic image quality is assessed using several parameters, including spatial resolution, contrast, noise, and artifacts. Among these parameters, the CNR plays a crucial role in determining CBCT image quality. CNR can be optimized by modifying various acquisition parameters, such as the FOV, kVp, and the number of basis images (25). However, these parameters were beyond the scope of the present study, and further research is warranted to investigate their potential effects.

Several limitations of the present study should be considered when interpreting the findings. In clinical practice, the maxillary and mandibular bones are surrounded by soft tissues, facial muscles, and skin, whereas this study was conducted using dry mandibles. Consequently, the findings may not fully represent the conditions encountered in actual patient CBCT images. Anatomical structures present in vivo may affect gray value measurements and the formation of artifacts. Furthermore, although experimental settings allow for controlled variables and accurate measurements, clinical practice involves various uncontrollable factors, such as patient movement, which may contribute to differences between experimental findings and clinical outcomes (19).

Conclusion

It seems that in addition to the type of amalgam, different exposure parameters and CBCT units play a role in the severity of artifacts caused by different amalgams. However, factors such as bone density may influence the severity of artifact, regardless of the amalgam type.

Declarations

Ethics approval and consent to participate

This study was conducted in accordance with the applicable institutional and ethical guidelines and was approved by the Ethics Committee of Babol University of Medical Sciences (Ethics approval code: IR.MUBABOL.HRI.REC.1403.125). No patient have been involved in this study.

The dry human mandibles used in this study were obtained from the Anatomy Department at Babol University of Medical Sciences, where consent from the next of kin for scientific research had been obtained previously. However, their identifying information remains confidential.

Conflict of Interest

The authors declare that they have no competing interests.

Funding

Not applicable.

Data Availability

The datasets used and/or analyzed during the current study are available from the corresponding author on reasonable request.

Author Contributions

Atena Jamali, Ehsan Moudi and Ariana Rezaei Majd contributed to the conception and design of the study, collection the study data, and writing the manuscript. Sina

Haghanifar, Homayoon Alaghehmand and Maryam Johari interpreted the study data. Ali Bijani analyzed the study data. Ehsan Moudi and Sina Haghanifar reviewed the article. All atthors contributed to critical review and final approval of the version to be published.

Consent for publication

Not applicable.

References

1. Hahn A, Knaup M, Brehm M, Sauppe S, Kachelrieß M. Two methods for reducing moving metal artifacts in cone-beam CT. Medical Physics. 2018;45(8):3671-80.

2. Safi Y, Ghazizadeh Ahsaie M, Jafarian Amiri M. Effect of the field of view size on CBCT artifacts caused by the presence of metal objects in the exomass. International journal of dentistry. 2022;2022(1):2071108.

3. Wajer R, Wajer A, Kazimierczak N, Wilamowska J, Serafin Z. The impact of AI on metal artifacts in CBCT oral cavity imaging. Diagnostics. 2024;14(12):1280.

4. Schulze R, Heil U, Groβ D, Bruellmann DD, Dranischnikow E, Schwanecke U, et al. Artefacts in CBCT: a review. Dentomaxillofacial Radiology. 2011;40(5):265-73.

5. Park HS, Seo JK, Hyun CM, Lee SM, Jeon K. A fidelity-embedded learning for metal artifact reduction in dental CBCT. Medical physics. 2022;49(8):5195-205.

6. Helvacioglu-Yigit D, Seki U, Kursun-Cakmak S, Demirturk Kocasarac H, Singh M. Comparative evaluation of artifacts originated by four different post materials using different CBCT settings. Tomography. 2022;8(6):2919-28.

7. Abdinian M, Hranadi MAT, Naeini MHM. Evaluating the effect of amalgam fillings on caries detection in cone-beam computed tomography images. Dental Research Journal. 2024;21(1):54.

8. Yamany I. A comparative analysis of different fields of view in cone beam computed tomography imaging to identify the inferior alveolar nerve canal: University of Connecticut; 2011.

9. Moudi E, Haghanifar S, Madani Z, Bijani A, Nabavi ZS. The effect of metal artifacts on the identification of vertical root fractures using different fields of view in cone-beam computed tomography. Imaging science in dentistry. 2015;45(3):147-51.

10. Gong X, Meyer E, Yu X, Sun J, Sheng L, Huang K, et al. Clinical evaluation of the normalized metal artefact reduction algorithm caused by dental fillings in CT. Dentomaxillofacial Radiology. 2013;42(4):20120105.

11. Farias-Gomes A, Fontenele RC, Rosado LPL, Neves FS, Freitas DQ. The metal post material influences the performance of artefact reduction algorithms in CBCT images. Brazilian Dental Journal. 2022;33:31-40.

12. Barrett JF, Keat N. Artifacts in CT: recognition and avoidance. Radiographics. 2004;24(6):1679-91.

13. Vahdani N, Moudi E, Ghobadi F, Mohammadi E, Bijani A, Haghanifar S. Evaluation of the metal artifact caused by dental implants in cone beam computed tomography images. Maedica. 2020;15(2):224.

14. Pauwels R, Stamatakis H, Bosmans H, Bogaerts R, Jacobs R, Horner K, et al. Quantification of metal artifacts on cone beam computed tomography images. Clinical oral implants research. 2013;24:94-9.

15. Gaêta-Araujo H, Nascimento EHL, Fontenele RC, Mancini AXM, Freitas DQ, Oliveira-Santos C. Magnitude of beam-hardening artifacts produced by gutta-percha and metal posts on cone-beam computed tomography with varying tube current. Imaging science in dentistry. 2020;50(1):1.

16. Siewerdsen JH, Moseley D, Bakhtiar B, Richard S, Jaffray DA. The influence of antiscatter grids on soft-tissue detectability in cone-beam computed tomography with flat-panel detectors: antiscatter grids in cone-beam CT. Medical physics. 2004;31(12):3506-20.

17. Schulze RKW, Berndt D, d'Hoedt B. On cone-beam computed tomography artifacts induced by titanium implants. Clinical oral implants research. 2010;21(1):100-7.

18. Oliveira ML, Tosoni GM, Lindsey DH, Mendoza K, Tetradis S, Mallya SM. Influence of anatomical location on CT numbers in cone beam computed tomography. Oral surgery, oral medicine, oral pathology and oral radiology. 2013;115(4):558-64.

19. Sabban H, Mahdian M, Dhingra A, Lurie AG, Tadinada A. Evaluation of linear measurements of implant sites based on head orientation during acquisition: an ex vivo study using cone-beam computed tomography. Imaging science in dentistry. 2015;45(2):73.

20. Chada R, Tahmasbi M, Nair M, Kesterke MJ, Jalali P. Beam hardening and scatter artifact with metal objects inside and outside the field of view in cone beam computed tomography (CBCT) imaging. Oral Surgery, Oral Medicine, Oral Pathology and Oral Radiology. 2025;139(3):e86-e7.

21. Schulze D, Heiland M, Blake F, Rother U, Schmelzle R. Evaluation of quality of reformatted images from two cone-beam computed tomographic systems. Journal of Cranio-Maxillofacial Surgery. 2005;33(1):19-23.

22. Machado AH, Fardim KAC, de Souza CF, Sotto-Maior BS, Assis NMSP, Devito KL. Effect of anatomical region on the formation of metal artefacts

produced by dental implants in cone beam computed tomographic images. Dentomaxillofacial Radiology. 2018;47(1):20170281.

23. Valizadeh S, Vasegh Z, Rezapanah S, Safi Y, Khaeazifard MJ. Effect of object position in cone beam computed tomography field of view for detection of root fractures in teeth with intra-canal posts. Iranian Journal of Radiology. 2015;12(4):e25272.

24. Min C-K, Kim K-A. Quantitative analysis of metal artefacts of dental implant in CBCT image by correlation analysis to micro-CT: A microstructural study. Dentomaxillofacial Radiology. 2021;50(3):20200365.

25. De Man B, Nuyts J, Dupont P, Marchal G, Suetens P, editors. Metal streak artifacts in X-ray computed tomography: a simulation study. 1998 IEEE Nuclear Science Symposium Conference Record 1998 IEEE Nuclear Science Symposium and Medical Imaging Conference (Cat No 98CH36255); 1998: IEEE.